

Supporting Information

Appendix S1 Description of how time- and depth-varying root biomass, soil organic matter, and microbial biomass carbon were estimated.

Root Carbon

Root biomass carbon (C_R) is expressed as the total amount of root biomass in a 1 m x 1 cm² column of soil (R^*) times the fraction of roots at each depth z , $f_R(z)$, scaled by an index of vegetation activity (greenness):

$$C_R(z, t) = R^* \cdot f_R(z) \cdot G(t)$$

where $G(t) = \left(1 + \frac{\text{Greenness}(t) - \text{mean}(\text{Greenness})}{\text{max}(\text{Greenness}) - \text{min}(\text{Greenness})}\right)$ and *Greenness* is vegetation greenness, which was estimated every 2-4 weeks between March and September by taking digital photographs using a 2 m high camera stand and a 1 m² ground frame; images were analyzed following methods described by Zelikova *et al.* (2015), and linear interpolations were used to estimate *Greenness* on non-measurement dates. The scaling by *Greenness* via $G(t)$ allows root C to vary over time (t), where the rate of change of *Greenness* is assumed as being a proxy for the rate of change of root biomass C. The calculation of *Greenness* results in this quantity (scaling factor) varying between ~0.5 and ~1.5 because the depth-varying measurements of root C mass were made in the middle of the growing season (Carrillo *et al.*, 2014). The function $R^* \cdot f_R(z)$ was estimated by fitting an exponential function, $R^* \exp(-z/\lambda)$, to site-level root biomass data collected at multiple depths (2.5, 10, 22.5, 37.5, 60, and 87.5 cm; Figure S4), where R^* and λ are parameters estimated via the fitting procedure. R^* represents the total amount of root C in the soil profile, while λ (estimate to be ~7) controls the slope of the curve (i.e., how fast root biomass decays with depth).

Soil Carbon and Microbial Biomass Carbon

A similar approach was used to describe how soil organic matter (SOM) carbon (C_{SOM}) and microbial biomass carbon (C_{MIC}) vary with depth. The depth distribution of SOM is described as:

$$C_{SOM}(z) = S^* \cdot f_S(z)$$

where $f_S(z)$ is an exponential decay function given by: $f_S(z) = \exp(-z/\lambda)$. We fit the exponential function to SOM data representing multiple depths (2.5, 10, 22.5 cm; Figure S4), giving an estimate of $\lambda=30$. A gamma distribution function was used to describe C_{MIC} such that

$$C_{MIC}(z) = M^* \cdot f_M(z)$$

$f_M(z) = \text{gampdf}(z, a, b)$, where *gampdf* is the gamma probability density function, as parameterized by Matlab. We fit the *gampdf* function to measurements of microbial biomass carbon also obtained for the same depths, leading to estimates of $a = 1.7$ and $b = 4.75$. As with root carbon, S^* and M^* represent the total SOM and total microbial biomass carbon in a 1 m x 1 cm² soil column. We assumed that the C_{SOM} and C_{MIC} profiles were invariant with time for the single growing season that we simulated.

Appendix S2 Calculation of initial conditions

The initial ($t = 0$) CO₂ concentration for at each depth z was calculated using the following function: $c(z,0) = 356 + (Q \cdot C_{max} z)/(Qz + C_{max})$, where C_{max} and Q are parameters that describe the curvature of the function, and z is the soil depth ($0 \text{ m} \leq z \leq 1 \text{ m}$). By informally fitting this equation to observations of soil CO₂ concentrations from 2007, taken from four different depths, we found that $C_{max} = 4500$ and $Q = 375$. See Figure S5 for the estimated versus observed CO₂ concentrations.

Figure S1 Differences in daily R_{soil} from DETECT for the soil texture scenario relative to the control

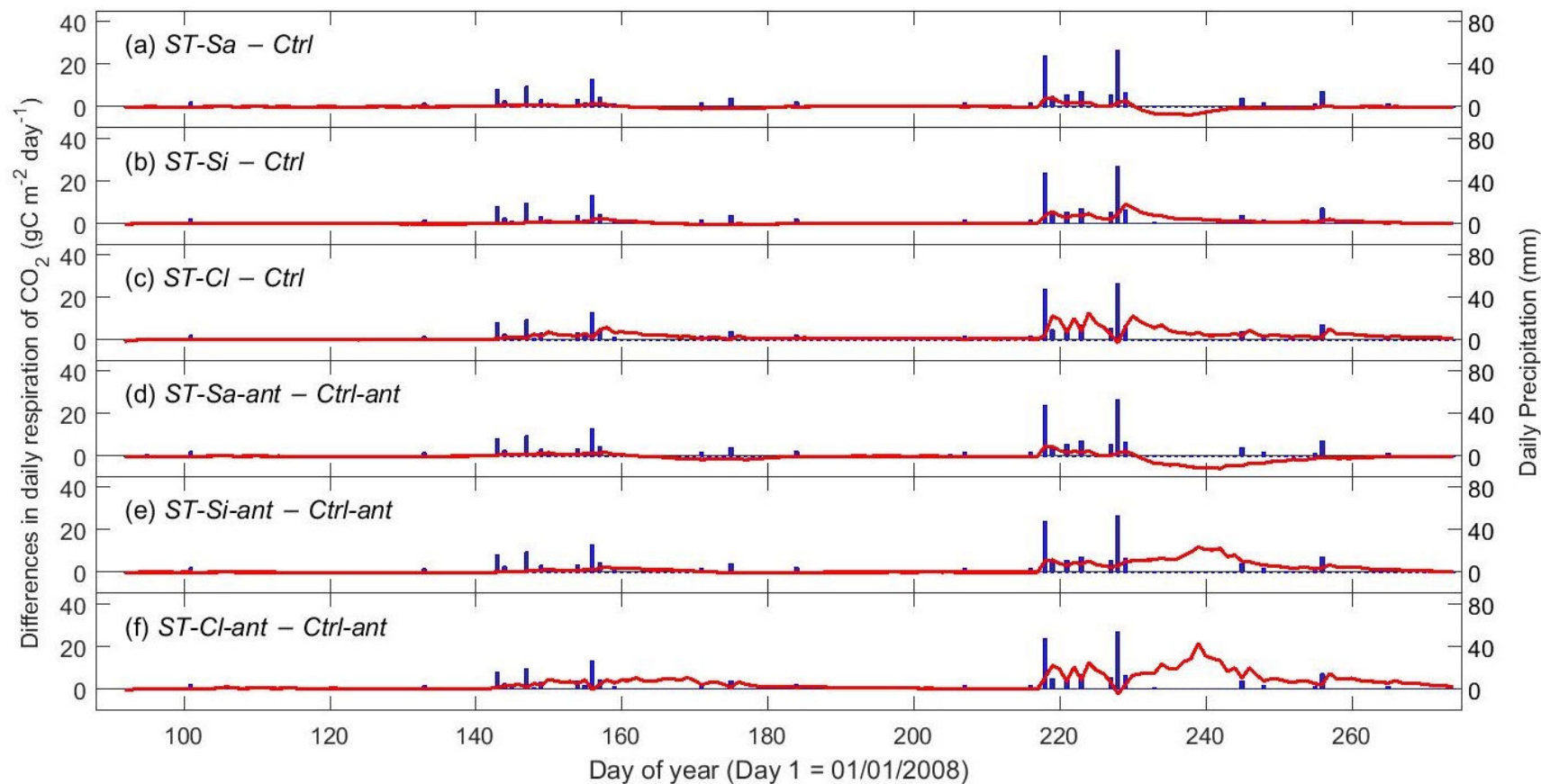


Figure S1 Panels (a), (b), and (c) show the time-series of the daily soil respiration (R_{soil}) from the non-steady state (DETECT) model for each soil texture scenario ($ST-Sa$, $ST-Si$, and $ST-Cl$) minus R_{soil} predicted by the DETECT model for the control scenario ($Ctrl$); all scenarios do not incorporate antecedent effects. Panels (d), (e), and (f) show the same as the first three panels, respectively, except that the antecedent version of the DETECT model is used for the control and soil texture scenarios ($Ctrl-ant$, $ST-Sa-ant$, $ST-Si-ant$, and $ST-Cl-ant$). See Table 2 in the main text for a description of the scenarios. Blue bars denote daily precipitation amounts.

Figure S2 Differences in daily R_{soil} from the antecedent versus non-antecedent versions of model under different precipitation scenarios

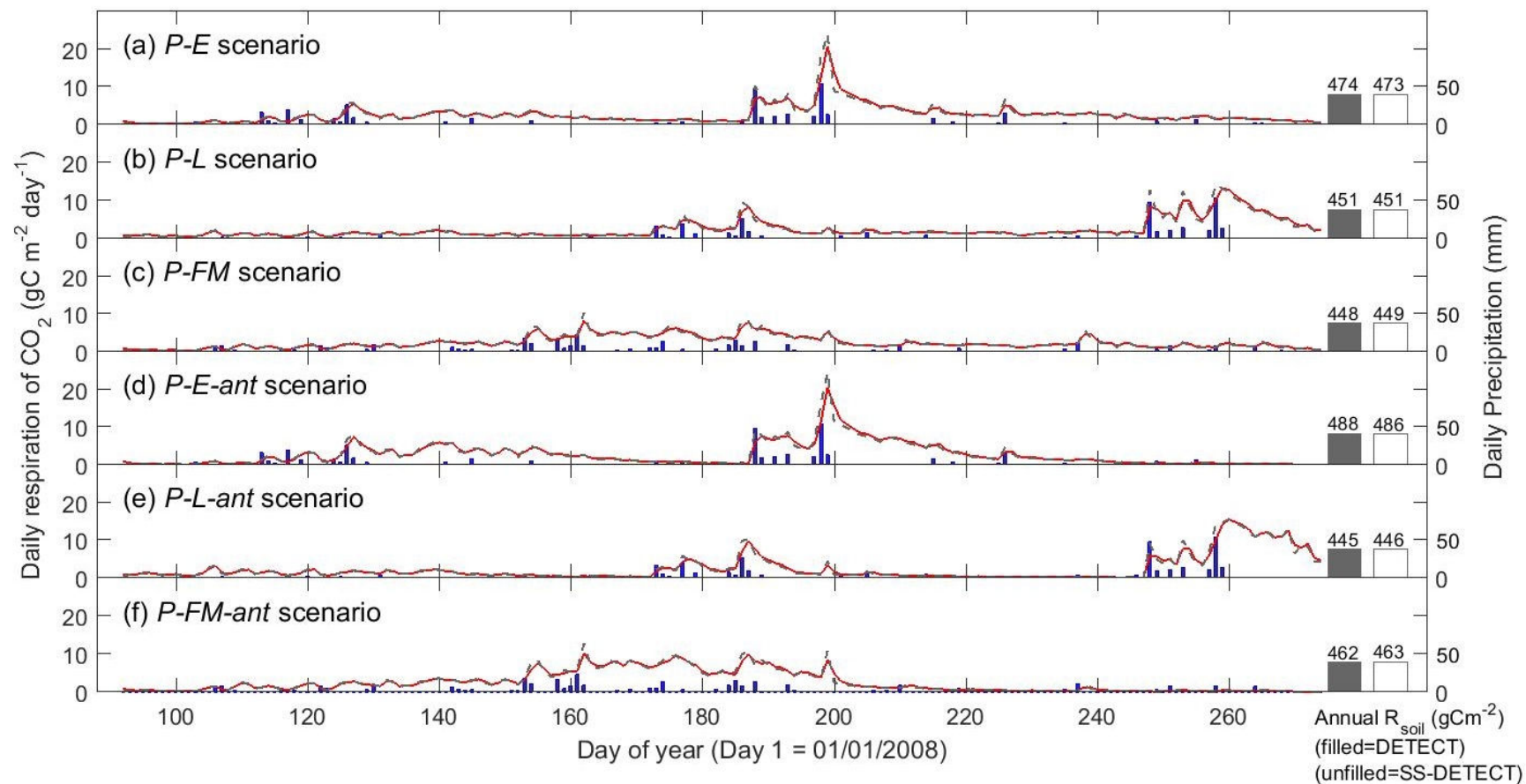


Figure S2 Time-series of daily soil respiration (R_{soil}) predicted from the non-steady-state (DETECT) and steady-state (SS-DETECT) models, for the precipitation scenarios using the non-antecedent (panels a, b, and c) and the antecedent (panels d, e, and f) parameterizations of the models. See Table 2 in the main text for a description of the scenarios. Blue bars denote daily precipitation amounts.

Figure S3a Predicted versus observed soil CO₂ concentrations (*Ctrl* scenario)

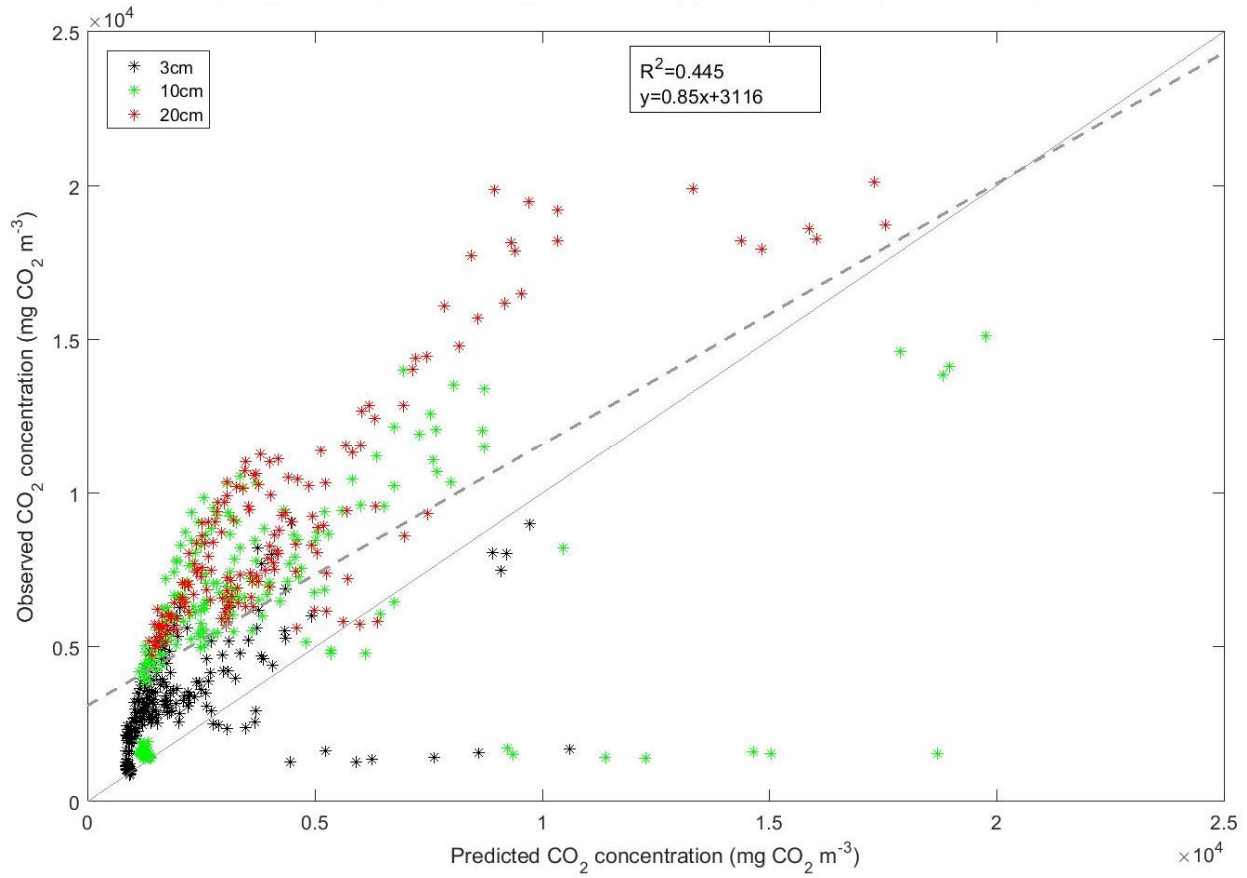


Figure S3a Predicted versus observed soil CO₂ concentrations, where the predictions are from the non-steady-state DETECT model used in the control (*Ctrl*) scenario, without antecedent effects. Observed soil CO₂ is based on soil gas probes installed at three depths (3, 10, and 20 cm) between April 1st and September 30th, 2008.

Figure S3b Predicted versus observed soil CO₂ concentrations (*Ctrl* and *Ctrl-ant* scenario)

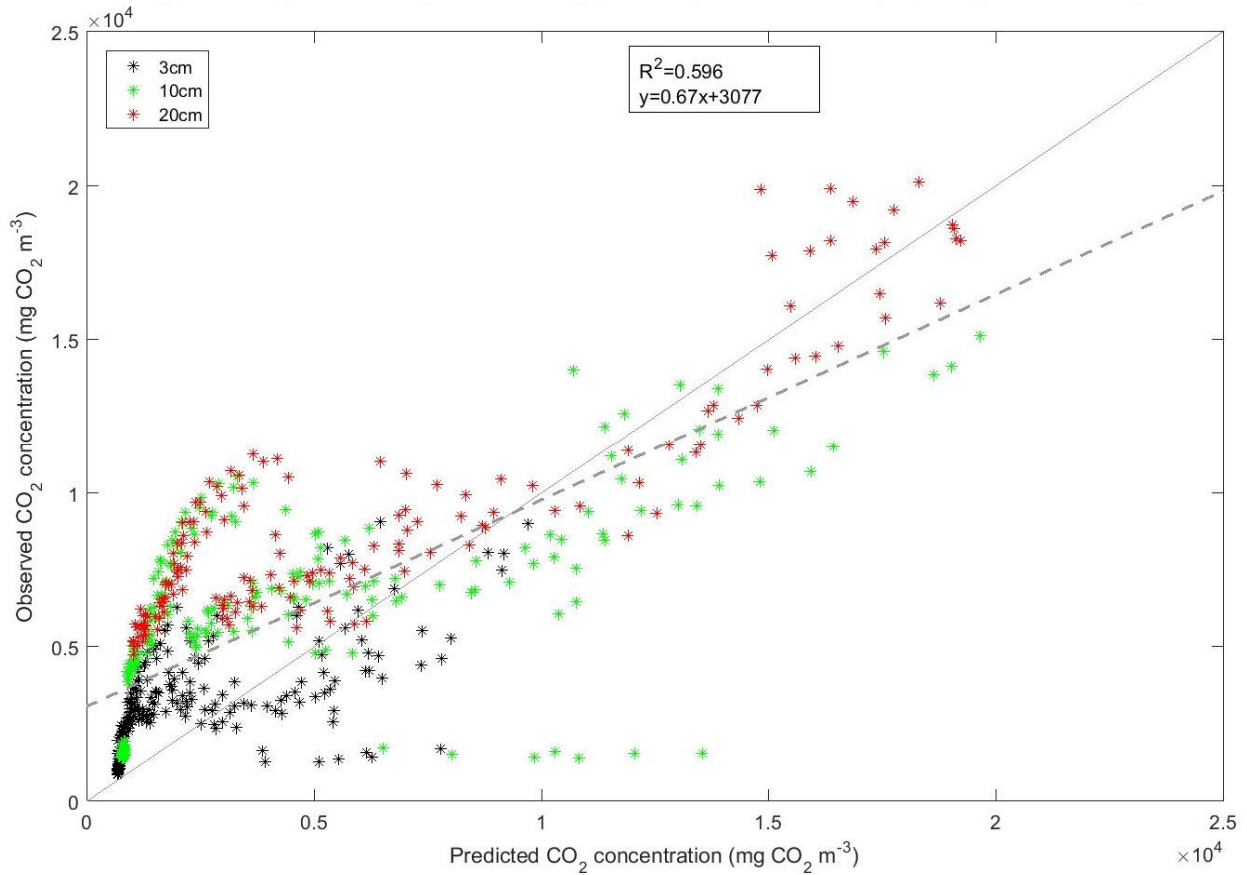


Figure S3b Predicted versus observed soil CO₂ concentrations, where the predictions are from the non-steady-state DETECT model used in the control scenario that includes antecedent soil water and temperature effects (*Ctrl-ant*). Observed soil CO₂ is based on soil gas probes installed at three depths (3, 10, and 20 cm) between April 1st and September 30th, 2008.

Figure S4

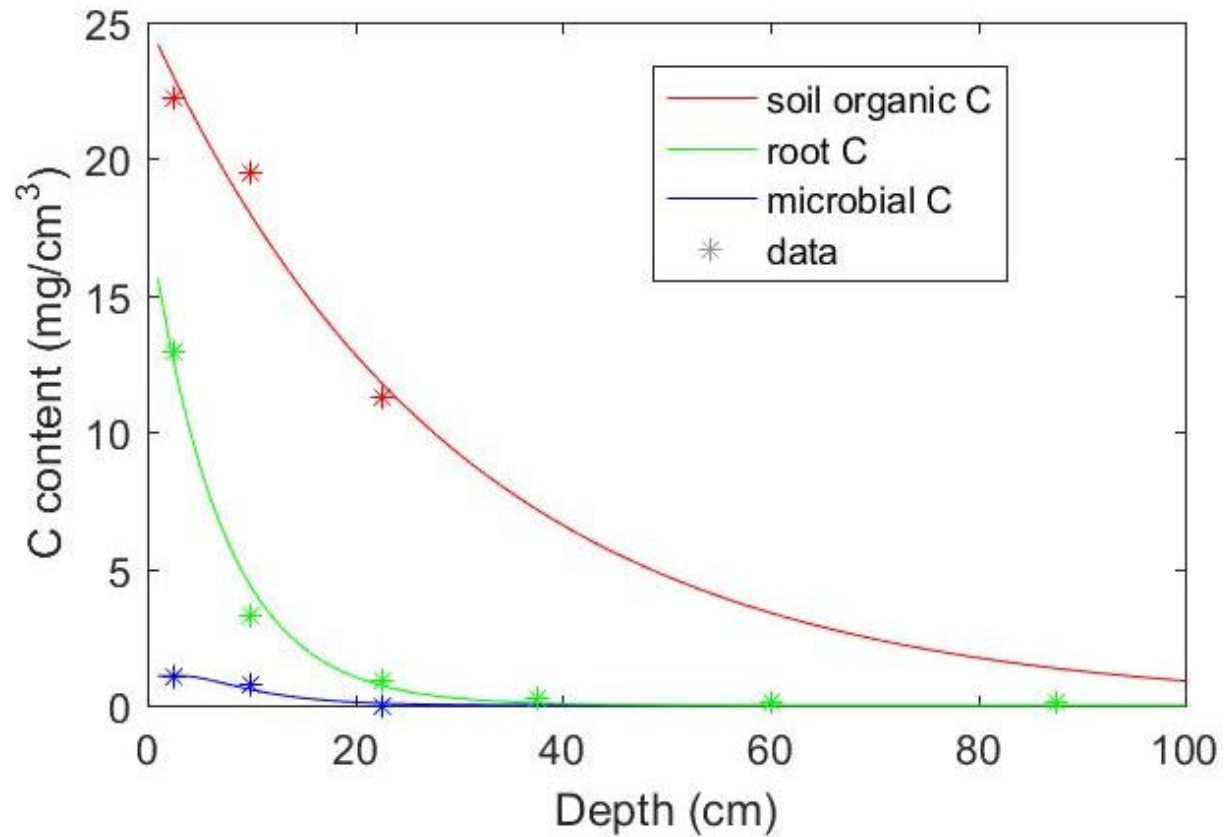


Figure S4 Observed versus estimated soil organic, root, and microbial carbon (C) with depth. The lines represent functions that were fit to the data to inform C_{SOM} , C_R , and C_{MIC} , respectively. See Appendix S1 for a description of the functions.

Figure S5

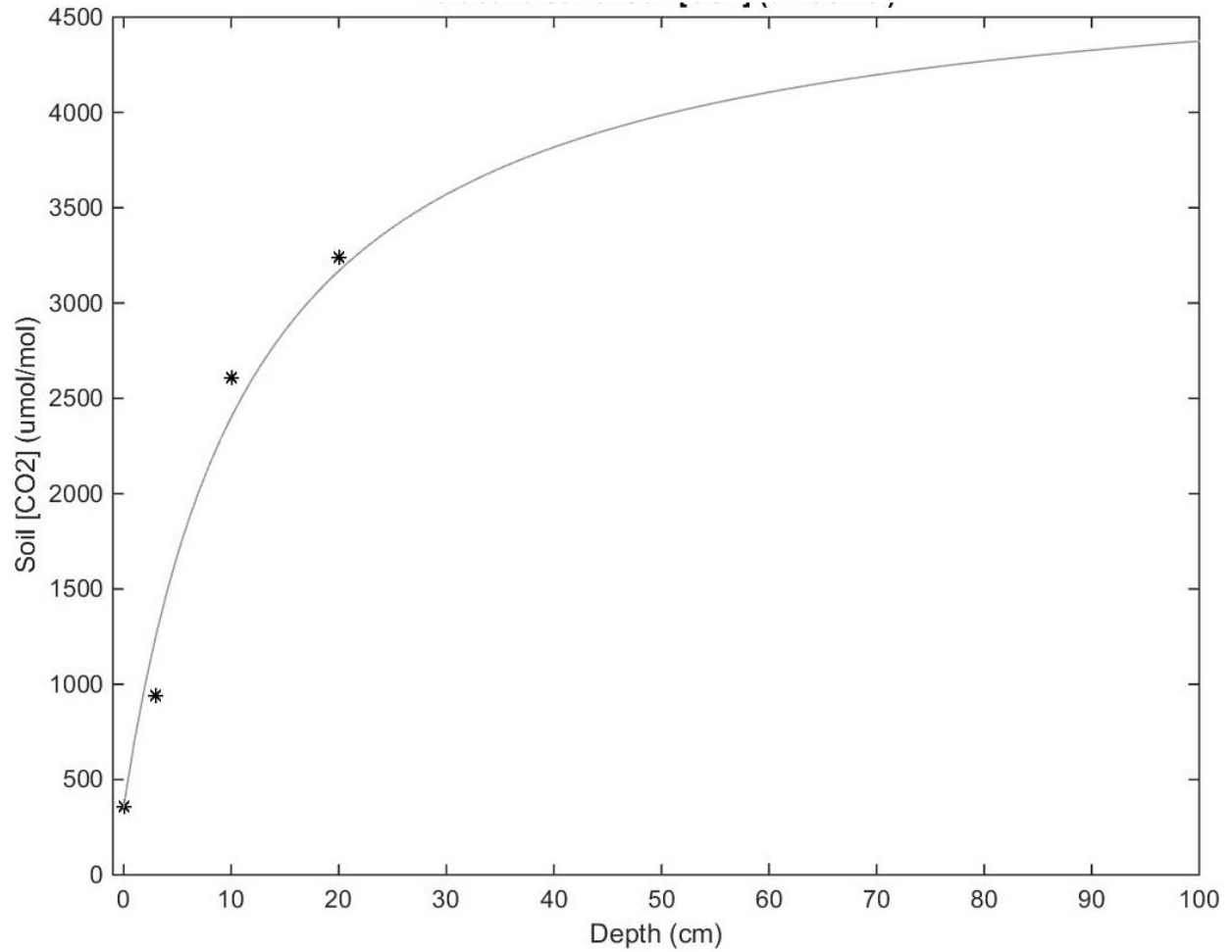


Figure S5 Observed (stars) versus modelled (curve) soil CO₂ concentrations with depth. The data for each of the four depths (0, 3, 10, and 20 cm) are averages of measured soil CO₂ concentrations taken at various points during the growing season of 2007. See Appendix S2 for a description of the function, which was used to inform the initial conditions, $c(z, 0)$.

Figure S6

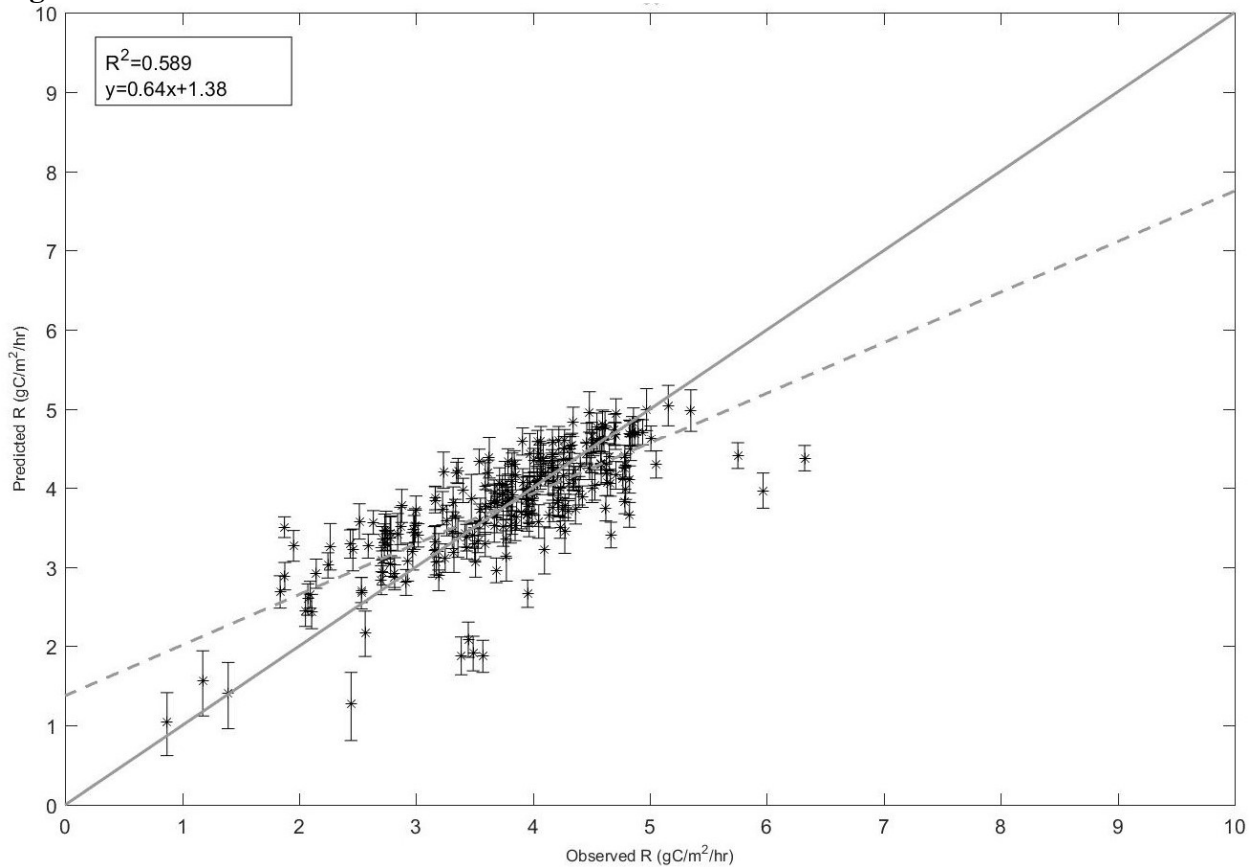


Figure S6 Observed surface-soil respiration derived from microbes (heterotrophs) from the PHACE experiment—based on ecosystem respiration measurements made on non-vegetated plots—versus predicted surface soil respiration due to microbes as informed by the microbial source term submodel (Eqn 5), but without the microbial C or CUE terms. The data were obtained by measuring the change in CO₂ concentration using a trace gas chamber, from a portion of each plot where herbicide was applied to remove all plant matter at the beginning of 2008. We assumed that during the first year after application of the herbicide, the microbes in the soil were respiring at the same rate as before the application. See Dijkstra et al. (2013) and Ogle et al. (2016) for details about the microbial respiration measurements and application of the herbicide.

References

Carrillo, Y., Dijkstra, F. A., LeCain, D., Morgan, J. A., Blumenthal, D., Waldron, S., and Pendall, E.: Disentangling root responses to climate change in a semiarid grassland, *Oecologia*, 2014. 1-13, 2014.

Dijkstra, F. A., Carrillo, Y., Pendall, E., and Morgan, J. A.: Rhizosphere priming: a nutrient perspective, *Frontiers in microbiology*, 4, 2013.

Ogle, K., Ryan, E., Dijkstra, F. A., and Pendall, E.: Quantifying and reducing uncertainties in estimated soil CO₂ fluxes with hierarchical data-model integration, *Journal of Geophysical Research: Biogeosciences*, 2016. 2016.

Zelikova, T. J., Williams, D. G., Hoenigman, R., Blumenthal, D. M., Morgan, J. A., and Pendall, E.: Seasonality of soil moisture mediates responses of ecosystem phenology to elevated CO₂ and warming in a semi-arid grassland, *Journal of Ecology*, 2015. 2015.